


## Construction of model Hamiltonians for transition-metal impurities via the quasiparticle self-consistent *GW* method

Harutaka Saito  and Katsuhiko Suzuki*Division of Materials and Manufacturing Science, Graduate School of Engineering, Osaka University, Suita, Osaka 565-0871, Japan*

Kazunori Sato

*Division of Materials and Manufacturing Science, Graduate School of Engineering, Osaka University, Suita, Osaka 565-0871, Japan; Center for Spintronics Research Network (CSRN), Osaka University, Toyonaka, Osaka 560-8531, Japan; and Spintronics Research Network Division, OTRI, Osaka University, Toyonaka, Osaka 560-8531, Japan*

Takao Kotani

*Advanced Mechanical and Electronic System Research Center, Department of Engineering, Tottori University, Tottori 680-8552, Japan and Center for Spintronics Research Network (CSRN), Osaka University, Toyonaka, Osaka 560-8531, Japan*

(Received 16 March 2023; revised 11 June 2023; accepted 6 July 2023; published 24 July 2023)

We show a method to construct model Hamiltonians for describing multiplet excitations of transition-metal impurities. Here, we treat systems of a transition metal substituting Al in  $\alpha$ -Al<sub>2</sub>O<sub>3</sub>. Based on the results of quasiparticle self-consistent *GW* (QSGW) calculations for the systems, we construct the model Hamiltonian of *3d* orbitals. We determine not only the crystal-field parameters, but also the parameters of effective interactions based on the theoretical correspondence between the QSGW calculations and the model Hamiltonian, and investigate the systematic change in these parameters. Finally, we discuss the structures of multiplet excitations calculated from these parameters.

DOI: [10.1103/PhysRevB.108.035141](https://doi.org/10.1103/PhysRevB.108.035141)

### I. INTRODUCTION

Light emission from luminescent centers of transition metals (TMs) is one of the most important physical phenomena for white light-emitting diode applications [1–6] as well as the tunable laser applications [7]. Ruby, Cr<sup>3+</sup>-doped  $\alpha$ -Al<sub>2</sub>O<sub>3</sub> ( $\alpha$ -Al<sub>2</sub>O<sub>3</sub>:Cr<sup>3+</sup>), was utilized for the first solid-state laser developed by Maiman [8].  $\alpha$ -Al<sub>2</sub>O<sub>3</sub>:Ti<sup>3+</sup> is widely used these days, whereas, other TM elements in  $\alpha$ -Al<sub>2</sub>O<sub>3</sub> are also potentially applicable to the solid-state lasers [9–12]. Possible combinations of TMs with host materials are extensively examined [7]. To assist such examination by the computational material design (CMD), we have to figure out a reliable method to compute properties that control the light emission. Such a method should be applicable to any systems on the same footing without choosing computational settings by hand.

The luminescent centers are described well as the multiplets of *3d* electrons. Excitations among these multiplets cause light emission. The spectrum of ruby is analyzed by the multiplet excitations [13,14]. If we assume the *3d* electrons of the luminescent center are well isolated from the other electrons, we can regard the system as TM *3d* electrons embedded in the crystal field (CF) with effective interactions between the electrons.

In order to treat the multiplets, we have to use a method to go beyond the mean-field theories, which describe electronic structure by a single Slater determinant. A possible method is based on the idea of the configuration interaction (CI) [15]. For instance, Cr<sup>3+</sup> in  $\alpha$ -Al<sub>2</sub>O<sub>3</sub> was examined by

the single-electron cluster calculation [16,17] where only a few positions of bands or lines of the spectrum were obtained from analytic relation between the molecular-orbital energies and the multiplet energies. Duan *et al.* calculated the whole multiplet structure of ruby, whereas, their method could not be applicable to the calculation of the emission spectra [18]. Also for  $\alpha$ -Al<sub>2</sub>O<sub>3</sub>:V<sup>3+</sup>, similar first-principles calculations were carried out [19,20]. Ogasawara *et al.* developed a hybrid method combining density functional theory (DFT) and the CI to obtain multiplet structures [21–23]. However, such methods based on CI have some problems to treat TM in solids. At first, we have to choose the size of clusters including TM at the center; such a choice is not easy technically, therefore, unsuitable for CMD. In addition, if the size of the cluster is not large enough, we may not reproduce properties of hosts, such as band gaps. This can cause a problem because we should describe the levels of *3d* electrons relative to the band structure of host materials so as to describe the localization of the *3d* electrons. In fact, we saw a large reduction of the spin-orbit coupling because of the delocalization of the *4f* eigenfunction when Eu is doped into GaN [24].

On the other hand, we may describe the electronic structure of the ground state even in a mean-field theory by a Slater determinant; in the case of atom, we expect that  $L_z$  and  $S_z$  of the Slater determinant should be consistent with the Hund rule. Kitaoka *et al.* performed the constraint DFT in the local spin density approximation (LSDA)+*U* resulting  $\sim 1.0$  eV for transition energy from <sup>4</sup>A<sub>2g</sub> to <sup>2</sup>E<sub>g</sub> states of  $\alpha$ -Al<sub>2</sub>O<sub>3</sub>:Cr<sup>3+</sup>, whereas, experimental value is around

1.8 eV [25]. Na-Phattalung *et al.* obtained the transition energies 2.12 eV between the  ${}^2E_g$  excited state and the  ${}^4A_{2g}$  ground state in the hybrid functional [26].

We have another first-principles approaches to determine only the parameters of CF. Haverkort *et al.* demonstrated *ab initio* cluster calculations including the full Coulomb interactions using the localized Wannier orbitals based on nonmagnetic generalized gradient approximation electronic structure [27]. Kuzian *et al.* performed calculations on local magnetic centers with open  $3d$  and  $5f$  shells using a similar Wannier orbital method [28]. Although their approaches gave good agreement with the experimental CF parameters, their methods are not satisfactory from the view of CMD because the adopted Coulomb parameters are those of free ion or experimental analysis.

In this paper, we present a method to determine the model Hamiltonian of  $3d$  electrons of the luminescent centers based on the quasiparticle self-consistent *GW* (QSGW) calculations [29–32]. This method, originally developed by Suzuki *et al.* [24] for  $4f$  multiplets, virtually overcomes problems in previous works mentioned above. The model Hamiltonian was constructed from the terms of the CF and the screened Coulomb interactions.

To determine the many-body model Hamiltonian (in other words, to determine parameters in the Hamiltonian) based on the one-body QSGW results, we start from our core idea. The core idea is in the requirement that “QSGW applied to the model Hamiltonian” should reproduce the one-body Hamiltonian of QSGW. This is possible because the idea of QSGW is applicable not only to the first-principles calculations, but also to the model Hamiltonians. This core idea satisfies a renormalization principle that the model Hamiltonian should be closer to the original Hamiltonian when we utilize larger model space, e.g., including electrons of ligands. Roughly speaking, QSGW is a screened Hartree-Fock method where the size of screening is self-consistently determined without parameters by hand. In the present paper, we adopted the QSGW method instead of the hybrid functional methods since QSGW incorporates fluctuations due to particle-hole excitations.

In practice, we use QSGW80 instead of QSGW. QSGW80 means that we use 80% QSGW + 20% LSDA for exchange-correlation terms. This is to avoid the overestimation of exchange effects due to the underestimation of screening effects for the interaction between electrons. A justification of QSGW80 is given in Ref. [33] where we show that the vertex correction adding to the random-phase approximation (RPA) used in QSGW enhances the screening effects by  $\sim 20\%$ . QSGW80 is a quick remedy including the vertex correction. We had observed that QSGW80 works well for a wide range of materials [32]. Applying QSGW80 to TM-doped  $\text{Al}_2\text{O}_3$  is justified by the fact that QSGW80 describes not only *sp*-block semiconductors/insulators, but also TM oxides very well. For instance, the spin-wave dispersions are well reproduced for TM and TM oxides [34,35]. We will show our results for TM-doped  $\alpha\text{-Al}_2\text{O}_3$  systematically in order to confirm the performance of our method.

In the next section, after showing computational setting of our first-principles calculations in Sec. II A, we will explain our model Hamiltonian  $\mathcal{H}$  specified by six parameters

in Sec. II B. Then, we will illustrate the determination of parameters in model Hamiltonian of  $3d$  orbitals in TMs in Sec. II C.

## II. METHOD

### A. First-principles calculations

$\alpha\text{-Al}_2\text{O}_3$  has a corundum structure: oxygen atoms around an aluminum ion are located at the vertices of a distorted octahedron. When an aluminum ion is substituted by a TM ion, its structure should be relaxed to become a more stable one. For structure optimization, we prepared a  $2\times 2\times 2$  rhombohedral supercell of  $\alpha\text{-Al}_2\text{O}_3$  substituted one aluminum ion with a TM ion for structure relaxation. Both the lattice volume and the atomic positions were optimized using the projected augmented-wave method with the revised Perdew-Burke-Ernzerhof functional for solids implemented in the QUANTUM ESPRESSO package [36,37]. The cut-off energy for wave functions is 60 Ry for the charge density, the potential is 360 Ry, and the  $k$ -point mesh is  $6\times 6\times 6$ . Since the optimized structure differs from the original one mainly around the TM ions, we extract the local  $1\times 1\times 1$  structure around the TM ion from the supercell and assume  $C_{3v}$  symmetry around the TM ion. This optimized crystal structure was employed for the QSGW80 calculation (see the results in Table SI of the Supplemental Material [38]). The charge neutrality is conserved by imposing uniform background charges to the cell: Positive (negative) charge  $+e$  ( $-e$ ) was added in the case of  $\text{TM}^{4+}$  ( $\text{TM}^{2+}$ ). On the contrary to the one-shot *GW*, the self-consistency cycle of QSGW automatically keeps the charge neutrality even with the background charge.

The first-principles QSGW calculations, as well as the local density approximation calculations for comparison, were performed with the ECALJ package in Ref. [39]. We used  $k$ -point mesh  $8\times 8\times 8$  for the band structure part, whereas,  $4\times 4\times 4$  for the self-energy part. We used  $10\times 10\times 10$  for producing maximally localized Wannier functions (MLWFs) of  $3d$  orbitals.

For calculations of free TM ions, we employed a face-centered-cubic structure with lattice constant 10 Å, which is sufficiently larger than the ionic radius of the TM free ion. Background charges were added to calculate the electronic states of TM cations. We used the same  $k$ -point mesh as in the cases of  $\alpha\text{-Al}_2\text{O}_3$ .

### B. Model Hamiltonian

In a similar manner with Ref. [24], we assume our model Hamiltonian ( $3d$  electrons only) as

$$\mathcal{H} = \mathcal{H}_0 + \mathcal{H}_{\text{CF}} + \mathcal{H}_{\text{C}}, \quad (1)$$

where we have  $\mathcal{H}_0$  for the spherical mean-field term,  $\mathcal{H}_{\text{CF}}$  for CF,  $\mathcal{H}_{\text{C}}$  for the effective Coulomb interaction. The dimension of  $\mathcal{H}$  is  ${}_{10}C_N$ , where  $N$  is the number of  $3d$  electrons, e.g.,  $N = 3$  for  $\text{Cr}^{3+}$  ( $3d^3$ ). Since we do not take into account hybridization with the other electrons, we put  $3d$  electrons at the zero level, that is, we set  $\mathcal{H}_0 = 0$ . The spin-orbit coupling is neglected because it affects little for the estimation of CF and the effective Coulomb parameters in the  $3d$  system.

$\mathcal{H}_{\text{CF}}$  and  $\mathcal{H}_{\text{C}}$  are given as

$$\mathcal{H}_{\text{CF}} = \mathcal{H}_{\text{CF}}^{C_{3v}} = \sum_{mm'} \sum_{\sigma\sigma'} (h_{\text{CF}}^{C_{3v}})_{mm'} \hat{c}_{m\sigma}^\dagger \hat{c}_{m'\sigma'}, \quad (2)$$

$$h_{\text{CF}}^{C_{3v}} = -7D\sigma O_2^0 - (14Dq + 21D\tau)O_4^0 + 2\sqrt{70}Dq(O_4^3 - O_4^{-3}), \quad (3)$$

$$\mathcal{H}_{\text{C}} = \frac{1}{2} \sum_{m_1 m_3} \sum_{m_2 m_4} \sum_{\sigma\sigma'} g_{m_1 m_2 m_3 m_4} \hat{c}_{m_1 \sigma}^\dagger \hat{c}_{m_2 \sigma'}^\dagger \hat{c}_{m_4 \sigma'} \hat{c}_{m_3 \sigma}. \quad (4)$$

Here,  $m$  and  $\sigma$  are for the magnetic quantum number and spin.  $\hat{c}_{m\sigma}$  is the electron-annihilation operator. We represent  $\mathcal{H}_{\text{CF}}$  with the Stevens' operator  $O_l^n$  [42], where we have the octahedral CF parameter  $Dq$ , the trigonal CF parameters  $D\sigma$  and  $D\tau$  [43] in addition because a TM ion replacing  $\text{Al}^{3+}$  in  $\alpha\text{-Al}_2\text{O}_3$  has  $C_{3v}$  symmetry.

$\mathcal{H}_{\text{C}}$  in Eq. (4) is given with

$$g_{m_1 m_2 m_3 m_4} = (-1)^{m_1 - m_3} \delta_{m_1 + m_2, m_3 + m_4} \times \sum_{p=0}^l F^{2p} c^{2p}(m_1, m_3) c^{2p}(m_2, m_4), \quad (5)$$

where we have the Gaunt coefficients  $c^p(m, m')$  and the Slater-Condon parameters  $F^{2p}$  [44].  $F^{2p}$  are given by the modified Slater-Condon parameters  $F_0$ ,  $F_2$ , and  $F_4$  [45] as

$$F^0 = F_0, \quad F^2 = 49F_2, \quad F^4 = 441F_4. \quad (6)$$

Note that  $U$  and  $J$  in Ref. [46] are related as  $U = F_0$  and  $J = (7/2)F_2 + (63/2)F_4$ .

As a summary,  $\mathcal{H}$  is determined by the six parameters,  $F_0$ ,  $F_2$ ,  $F_4$ ,  $Dq$ ,  $D\sigma$ , and  $D\tau$  via  $\mathcal{H}_{\text{C}}$  and  $\mathcal{H}_{\text{CF}}$ . As shown in Sec. II C, we can determine the six parameters by our matching method after we perform QSGW80 calculations for  $\alpha\text{-Al}_2\text{O}_3\text{:TMs}$ .

### C. Determination of parameters in the model Hamiltonian

Based on the core idea given in the Introduction, we have to determine the six parameters so that the one-body Hamiltonian of QSGW for  $3d$  electrons  $\mathcal{H}_{\text{QSGW}}^{3d}$  is reproduced when we apply QSGW to  $\mathcal{H}$ . Note that we can apply QSGW even to the model Hamiltonian.

Now, we make a further approximation for simplicity. We first apply the first-principles method, QSGW80 to the systems where we substitute one of the Al sites in the host material  $\alpha\text{-Al}_2\text{O}_3$  with one TM ion. From this result of QSGW80, we obtain  $\mathcal{H}_{\text{QSGW}}^{3d}$  in the procedure of the MLWFs [47]. We expect QSGW80 gives a good description of the screening effect [33]. Then, we determine the six parameters so that  $\mathcal{H}_{\text{QSGW}}^{3d}$  is reproduced well using the result calculated by the Hartree-Fock approximation (HFA) applied to  $\mathcal{H}$ . We assume that applying HFA to  $\mathcal{H}$  with the screened Coulomb parameters gives virtually the same results as applying QSGW to  $\mathcal{H}$ . We think this assumption is reasonable since QSGW can be interpreted as a Hartree-Fock method with the screened Coulomb interaction instead of the bare one.

Let us illustrate the case of  $\text{Al}_2\text{O}_3\text{:Cr}^{3+}$ . In Figs. 1(b) (majority spin) and 1(e) (minority spin), we show the band

structure of  $\alpha\text{-Al}_2\text{O}_3\text{:Cr}^{3+}$  in QSGW80 together with that in LSDA as references [(a) and (d)]. We use a supercell of  $\alpha\text{-Al}_2\text{O}_3$  with one Cr substituting Al (see Fig. S1 in the Supplemental Material [38]). QSGW80 gives the band gap of 9.2 eV for  $\text{Al}_2\text{O}_3$ , in good agreement with experimental value (8.7 eV [48]), whereas, LSDA gives too small a value 6.5 eV. Impurity levels of  $3d$  orbitals relative to the host bands can affect the localization of the  $3d$  orbitals and hybridization with host electrons. QSGW80 is one of the best available choices to obtain band gaps as well as the impurity levels correctly. In Ref. [32], we see how QSGW80 works not only for simple insulators, but for NiO and MnO. We, therefore, use QSGW80 in order to describe both transition-metal compounds and semiconductors/insulators on the same footing.

In the left panels of Figs. 1(c) and 1(f) (the MLWF panels), we show ten eigenvalues (five for each spin) of  $\mathcal{H}_{\text{QSGW}}^{3d}$ , which is calculated in the manner of MLWFs for the results of QSGW80. We see  $t_{2g}$  states are almost degenerated,  $e_g$  states as well. This means that octahedral symmetry is almost preserved.  $\mathcal{H}_{\text{QSGW}}^{3d}$  is, thus, specified essentially by three levels relative to the occupied  $t_{2g}$  states of majority spin.

The HFA to  $\mathcal{H}$  gives the one-body Hamiltonian  $\mathcal{H}_{\text{HF}}$  as

$$\begin{aligned} \mathcal{H}_{\text{HF}} &= \mathcal{H}_{\text{CF}} + \mathcal{H}_{\text{C}}^{\text{HF}}, \\ \mathcal{H}_{\text{C}}^{\text{HF}} &= \sum_{m_1 m_3} \sum_{\sigma} \left[ \sum_{m_2 m_4} (g_{m_1 m_2 m_3 m_4}^{\sigma\sigma} - g_{m_1 m_2 m_4 m_3}^{\sigma\sigma}) (c_{m_2 \sigma}^\dagger c_{m_4 \sigma}) \right. \\ &\quad \left. + g_{m_1 m_2 m_3 m_4}^{\sigma\bar{\sigma}} (c_{m_2 \bar{\sigma}}^\dagger c_{m_4 \bar{\sigma}}) \right] \hat{c}_{m_1 \sigma}^\dagger \hat{c}_{m_3 \sigma}. \end{aligned} \quad (7)$$

Here,  $\bar{\sigma}$  is opposite spin to  $\sigma$ .  $\langle \dots \rangle$  is the expectation value for the ground state. We name  $\mathcal{H}_{\text{HF}}$  the Hartree-Fock model Hamiltonian (HFMH). We determine the six parameters so that  $\mathcal{H}_{\text{HF}}$  is in agreement with  $\mathcal{H}_{\text{QSGW}}^{3d}$  as good as possible, without paying attention to the matrix elements. Since  $\mathcal{H}_{\text{QSGW}}^{3d}$  has the freedom of a five-dimensional Hermitian matrix for each spin, we cannot expect perfect agreement.

We have to determine the six parameters so as to minimize the mean-square error between  $\mathcal{H}_{\text{HF}}$  and  $\mathcal{H}_{\text{QSGW}}^{3d}$  using the Powell's optimization method implemented in SCIPY. Here, we only require that  $\mathcal{H}_{\text{HF}}$  should reproduce these ten eigenvalues of  $\mathcal{H}_{\text{QSGW}}^{3d}$  as good as possible. This is because the matching of eigenvalues is the main part of the minimization; we guess that it is not meaningful to consider the matching of matrix elements within our current model of  $3d$  only. Our minimization virtually gives  $D\sigma = D\tau = 0$  for  $\text{Al}_2\text{O}_3\text{:Cr}^{3+}$  because of the almost-preserved octahedral symmetry. Two degrees of freedom due to  $10Dq$  and  $F_0$ , are not enough to reproduce the three levels. Thus, we need two more contributions due to  $F_2$  and  $F_4$ . In Figs. 1(c) and 1(f) (the HFMH panels), we resolve contributions from  $F_0$ ,  $F_2$ ,  $F_4$ , and  $10Dq$ . We see that the degeneracy of octahedral symmetry is preserved well. In Fig. 1(c), we see that the degeneracy of occupied states of the majority spin is recovered by adding the contribution from  $F_4$ , although the degeneracies of other states are not completely recovered because of our limited degree of freedom. As shown in Table I,  $D\sigma$  and  $D\tau$  are essentially needed in cases, especially for the cases of Fe, Ni, and Cu.

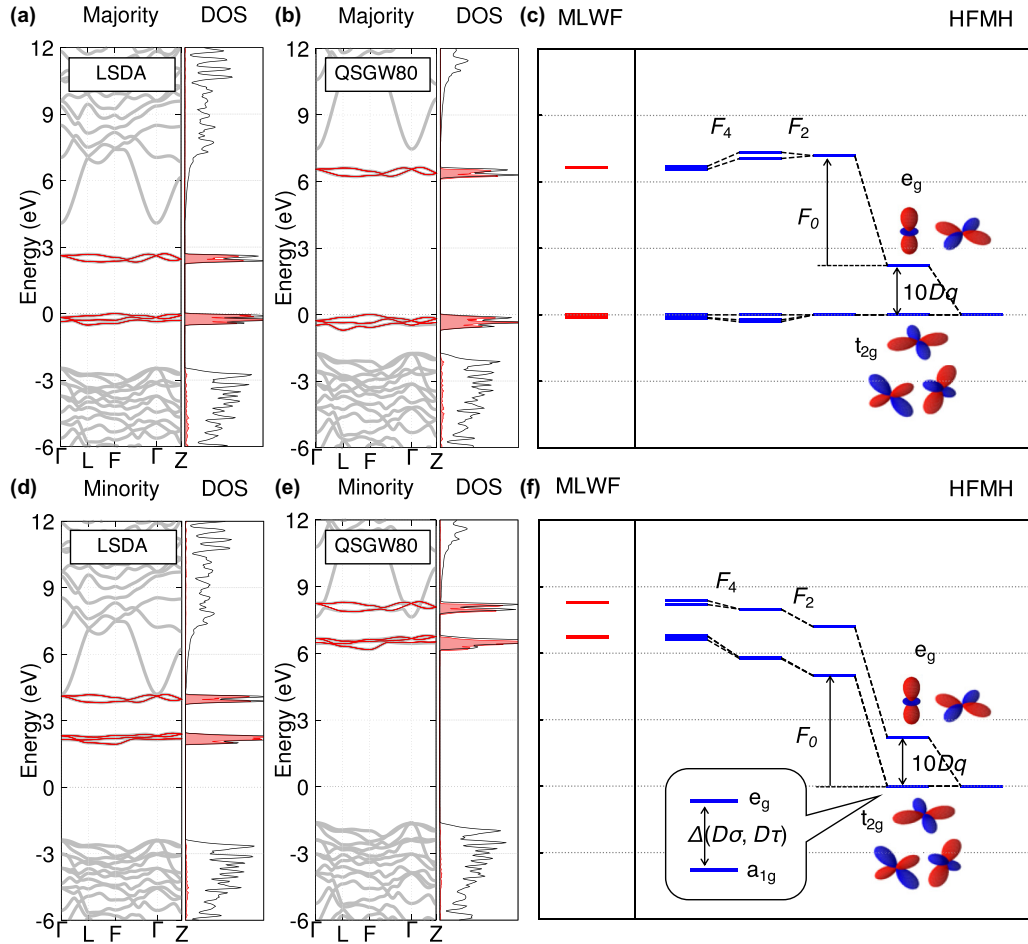


FIG. 1. The electronic structure and parameter determination of  $\alpha\text{-Al}_2\text{O}_3\text{:Cr}^{3+}$ . (a) and (d): The band structure of majority and minority spins together with density of states (DOS) calculated in LSDA. The red lines are for the MLWFs of Cr  $3d$  orbitals. The red filled region is for the partial DOS of Cr  $3d$ ; (b) and (e): in QSGW80; (c) and (f): The red lines in the left panel of (c) and (f) (MLWF panel) show the eigenvalues of  $\mathcal{H}_{\text{QSGW}}^{3d}$  (see the text). In the right panel [HFMH panel], the contributions of six parameters are resolved (see the text). Inset illustrates  $D\sigma$  and  $D\tau$  split  $t_{2g}$  into  $e_g$  and  $a_{1g}$ .

In Sec. III A, we will show our main results of the six parameters of TMs in  $\alpha\text{-Al}_2\text{O}_3$ . To have a better understanding of the results, we will show the calculated parameters of free ions in Sec. III B.

### III. RESULTS AND DISCUSSION

#### A. Calculated parameters in the model Hamiltonian

In Table I, we show calculated six parameters in  $\mathcal{H}$  for  $\text{TM}^{2+}$ ,  $\text{TM}^{3+}$ , or  $\text{TM}^{4+}$  in  $\alpha\text{-Al}_2\text{O}_3$  together with the experimental ones derived from optical measurements. In cases of  $\text{Fe}^{3+}$ , we have two results corresponding to two converged results of QSGW, the high spin (HS) and the low spin (LS) states. In cases shown in square brackets such as  $[\text{Fe}^{3+}(d^5)\dots]$ , we found that  $3d$  occupied states are strongly hybridized with the oxygen  $2p$  orbitals. Our current model including only  $3d$  orbitals may not be suitable enough for such cases. Thus, data lines with square brackets should be taken as less reliable cases. The calculated DOS in the Supplemental Material shows the size of hybridization (Figs. S2–S8) [38].

For  $\text{Cr}^{3+}$ ,  $F_0 = 4.98$  eV in QSGW80 is very different from 0.80 eV in LSDA. This is because LSDA does not include

on-site nonlocality of the one-body potential, which is usually described by  $U$  of LSDA+ $U$ . This causes the difference of positions of  $3d$  bands (see Fig. 1 in Sec. II). On the other hand, we see just  $\sim 10\%$  differences as for  $F_2$ ,  $F_4$ , and  $10Dq$  between QSGW80 and LSDA. This means that difference in the screening effects given in QSGW80 and in LSDA does not affect the anisotropic part of interactions so much.  $F_2 = 0.108$  eV in QSGW80 gave a little better agreement with experimental values 0.136 or 0.133 eV than  $F_2 = 0.092$  eV in LSDA. Since we usually expect that varieties of experimental values fall between QSGW80 and LSDA, we feel still the remaining difference of  $0.136 - 0.108 = 0.028$  eV sounds a little too large, whereas, we have no definite idea to identify the main cause of the difference. A cluster theory [23] shows better agreement with experiments, however, it is not simple enough as a method for CMD. Note that we cannot determine  $F_2$  and  $F_4$  for the case where all of the majority spin states are filled completely (HS with  $d^5$ ) because degeneracy of  $3d$  bands in QSGW80 gives insufficient information for determining all the six parameters. We have room to improve this point by adding bias fields in QSGW80 to have the information of the excited states as well.

TABLE I. Calculated six parameters of TM ions in  $\alpha$ -Al<sub>2</sub>O<sub>3</sub>. The number of  $3d$  occupancy is shown as  $d^m$  ( $m = 1, \dots, 9$ ).  $N_{\uparrow} - N_{\downarrow}$  means the spin moment in  $\mu_B$ . HS is for high spin, LS is for low spin. Some of “—” for  $d^5$  mean no data in our current treatment. The systems with brackets means strong hybridization with  $2p$  orbitals (see the text).

TM ion	$N_{\uparrow} - N_{\downarrow}$	Method	$F_0$ (eV)	$F_2$ (eV)	$F_4$ (eV)	$10Dq$ (eV)	$D\sigma$ (eV)	$D\tau$ (eV)
Ti <sup>2+</sup> ( $d^2$ )	2	QSGW80	4.46	0.093	0.0070	2.68	−0.005	0.000
V <sup>2+</sup> ( $d^3$ )	3	QSGW80	4.92	0.087	0.0104	2.64	−0.001	0.001
		Expt. [49]		0.112	0.0088	1.69	0.048	−0.022
Cr <sup>2+</sup> ( $d^4$ ) HS	4	QSGW80	5.50	0.166	0.0081	2.10	0.281	−0.023
		Expt. [50]		0.118	0.0096	1.86		
Cr <sup>2+</sup> ( $d^4$ ) LS	0	QSGW80	4.44	0.250	0.0135	2.35	0.029	0.009
Mn <sup>2+</sup> ( $d^5$ ) HS	5	QSGW80	9.55	—	—	1.82	—	—
		Expt. [51]		0.149	0.0127	1.25		
Mn <sup>2+</sup> ( $d^5$ ) LS	1	QSGW80	4.92	0.089	0.0142	2.41	−0.015	0.004
Fe <sup>2+</sup> ( $d^6$ ) HS	4	QSGW80	5.78	0.151	0.0148	1.97	0.144	−0.030
[Co <sup>2+</sup> ( $d^7$ ) HS	3	QSGW80	6.00	0.195	0.0119	2.11	0.000	0.000]
		Expt. [52]		0.167	0.0131	1.37		
[Ni <sup>2+</sup> ( $d^8$ )	2	QSGW80	5.49	0.142	0.0130	2.44	0.004	0.007]
		Expt. [53]		0.187	0.0151	1.25		
[Cu <sup>2+</sup> ( $d^9$ )	1	QSGW80	5.54	0.220	0.0112	2.13	−0.115	−0.008]
Ti <sup>3+</sup> ( $d^1$ )	1	QSGW80	4.59	0.095	0.0124	2.73	0.004	−0.001
		Expt. [54]				2.36		
V <sup>3+</sup> ( $d^2$ )	2	QSGW80	4.77	0.117	0.0099	2.40	−0.003	0.003
		Expt. [55]		0.129	0.0093	2.21	0.002	−0.013
Cr <sup>3+</sup> ( $d^3$ )	3	QSGW80	4.98	0.108	0.0113	2.17	−0.001	0.001
		LSDA	0.80	0.092	0.0105	2.33	0.003	0.000
		Theory[23]		0.123	0.0099	2.27		
		Expt. [57]		0.136	0.0131	2.32	−0.057	−0.012
		Expt. [14]		0.133	0.0106	2.25		
Mn <sup>3+</sup> ( $d^4$ ) LS	0	QSGW80	4.15	0.256	0.0112	2.04	−0.021	0.005
Fe <sup>3+</sup> ( $d^5$ ) LS	1	QSGW80	4.00	0.141	0.0054	1.25	−0.199	0.013
[Fe <sup>3+</sup> ( $d^5$ ) HS	5	QSGW80	10.6	—	—	1.19	—	—]
		Expt. [51]		0.137	0.0111	1.87		
[Co <sup>3+</sup> ( $d^6$ ) HS	4	QSGW80	5.06	0.170	0.0150	1.19	−0.133	0.021]
[Ni <sup>3+</sup> ( $d^7$ ) HS	3	QSGW80	5.72	0.129	0.0107	1.21	−0.152	0.027]
[Ni <sup>3+</sup> ( $d^7$ ) LS	1	QSGW80	3.36	0.190	0.0110	3.01	−0.015	−0.029]
V <sup>4+</sup> ( $d^1$ )	1	QSGW80	3.85	0.116	0.0132	2.68	0.021	−0.002
		Expt. [58]				2.48		
Cr <sup>4+</sup> ( $d^2$ )	2	QSGW80	3.61	0.119	0.0116	2.52	0.010	0.000
		Expt. [59]		0.139	0.0113	2.67	−0.022	−0.013
[Mn <sup>4+</sup> ( $d^3$ )	3	QSGW80	5.56	0.103	0.0124	2.23	0.006	−0.001]
		Expt. [49]		0.162	0.0099	2.69	−0.001	−0.026]
[Fe <sup>4+</sup> ( $d^4$ ) LS	2	QSGW80	3.60	0.141	0.0100	2.12	0.000	0.000]
[Co <sup>4+</sup> ( $d^5$ ) HS	5	QSGW80	6.87	—	—	1.33	—	—]
[Co <sup>4+</sup> ( $d^5$ ) LS	1	QSGW80	3.34	0.226	0.0124	2.57	−0.503	0.051]

Let us compare our results of QSGW80 with experimental analysis. In the cases of V<sup>3+</sup> as well as Cr<sup>4+</sup>, we see good agreement as in Cr<sup>3+</sup>. To make an overall comparison, we plot the data in Table I (only lines without square brackets) in Figs. 2(a)–2(d).  $F_0$  shows monotonic behavior except  $d^5$  where we have fewer screening effects due to the missing of spin-preserving transitions among  $3d$  electrons. For  $F_2$  in cases without square brackets, we have agreements within  $\sim 20\%$ . For example, V<sup>2+</sup> for  $F_2$  has agreement with the difference only 0.112 eV(Expt.)/0.087 eV(QSGW80). We see similar agreements for  $F_4$ . On the other hand, the experimental  $10Dq$  for TM<sup>2+</sup> shows too large a difference; the experimental

value is only  $\sim 70\%$  of QSGW values; 1.69 eV/2.64 eV for V<sup>2+</sup> and 1.25 eV/1.82 eV for Mn<sup>2+</sup>. A reason might be in the background charge used for our supercell (see Sec. II A) to keep the given valency. In fact, we may expect TM<sup>2+</sup> replacing Al<sup>3+</sup> should introduce one half of oxygen vacancy near TM<sup>2+</sup>. This may reduce the octahedral symmetry, resulting in smaller  $e_g$ - $t_{2g}$  splitting effectively.

We calculated the multiplet excitation energies by the exact diagonalization of  $\mathcal{H}$  [56] with the parameters in Table I. Figure 3 is the Tanabe-Sugano diagram of  $\alpha$ -Al<sub>2</sub>O<sub>3</sub>:Cr<sup>3+</sup>, showing multiplet energies relative to the ground state  ${}^4A_{2g}$  as a function of  $10Dq$ . We show a label of multiplet for

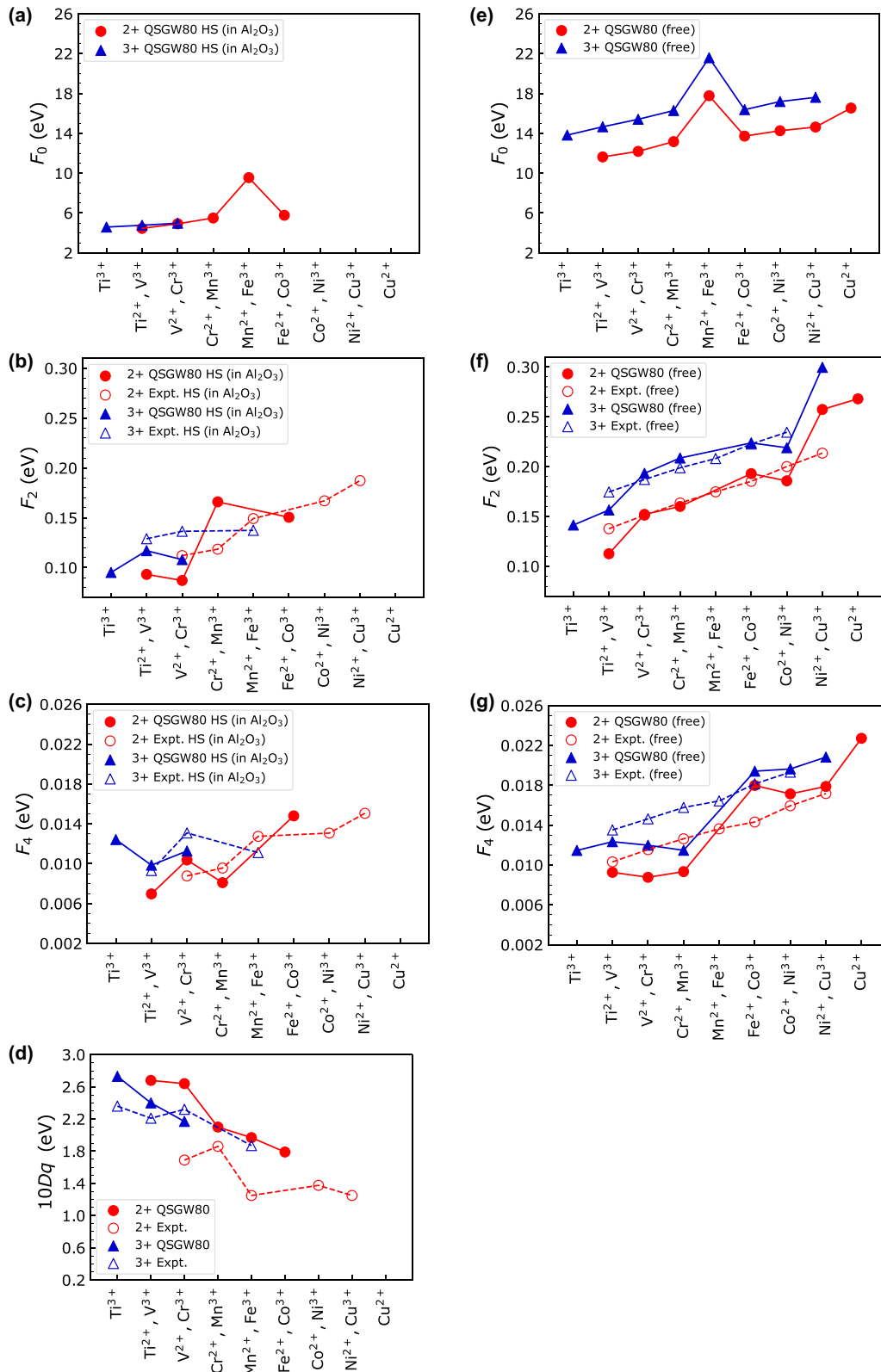


FIG. 2. The parameters of effective Coulomb interactions and cubic CF interaction as a function of the 3d electron number in  $\alpha\text{-Al}_2\text{O}_3$  compared with those in free ions. The trends of four parameters are shown in (a) and (e): The modified Slater-Condon parameter  $F_0$ ; (b) and (f):  $F_2$ ; (c) and (g):  $F_4$ ; and (g): cubic CF parameter  $10Dq$ . The left figures show results of TM ions in  $\alpha\text{-Al}_2\text{O}_3$ , and the right show results of the ones of free TM ions. In all the figures, the following symbols are employed: red circles denote the QSGW80 of  $\text{TM}^{2+}$ , blue triangles denote the QSGW80 of  $\text{TM}^{3+}$ , and open symbols express experimental analysis. Circles express  $\text{TM}^{2+}$ , and triangles express  $\text{TM}^{3+}$ .

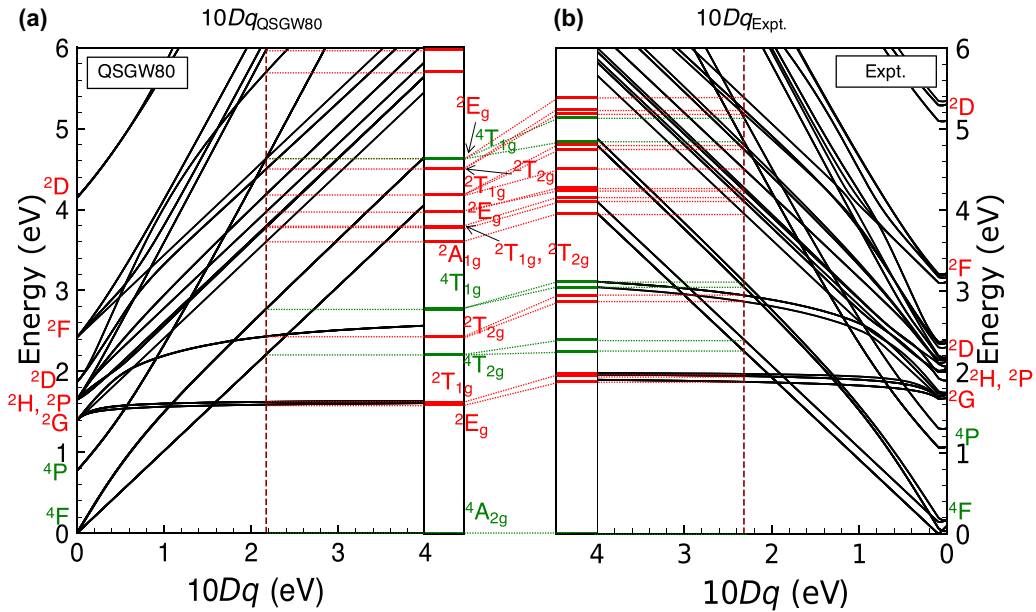


FIG. 3. Tanabe-Sugano diagram of  $\text{Cr}^{3+}$  in  $\alpha\text{-Al}_2\text{O}_3$  ( $d^3$ ). (a): Calculation results by using the parameters given by the QSGW80. The axis  $10Dq = 0$  roughly corresponds to the energy splitting of free ion states, namely, multiplet structure without CF parameters. Multiplet symbols are assigned to each state, and these are distinguished by spin multiplicity of doublet (red) and quartet (green). The symbols of irreducible representation of  $O_h$  symmetry are shown in the QSGW80 multiplet structure. The red broken line means the  $10Dq$  value of the QSGW80. The intersection points of this red broken line and black curves give multiplet states. (b): Result of experimental analysis. The horizontal axis in (b) is opposite to that in (a). Corresponding multiplet states between (a) and (b) are connected by dotted lines.

each branch. Figure 3(a) is for the set of parameters of the QSGW80, Fig. 3(b) is for the set of the experimental analysis [57] as well. We see how the difference in the sets results in the difference of the multiplet excitations. Because of the non-negligible size of  $D\sigma = -0.057$  eV, Fig. 3(b) shows minor splittings of branches as well as kinky behaviors of branches near  $10Dq = 0$ , whereas Fig. 3(a) does not show them.

Considering the fact that  $10Dq$ 's are similar in Figs. 3(a) and 3(b), differences of excitation energies should be mainly from  $F_2$  and  $F_4$ . In fact, the difference of excitation energies ( $\sim 20\%$ ) is almost corresponding to the error ratio of  $F_2$  between experimental analysis and QSGW80,  $(0.136 - 0.108)/0.136 \sim 0.21$ , and that of  $F_4$ ,  $(0.131 - 0.113)/0.113 \sim 0.15$ . In contrast, we see quartets  $^4T_{2g}$  and  $^4T_{1g}$  shown by green are less affected by the ratio. Only multiplets starting from  $^2G$  show strong nonlinear behaviors as a function of  $10Dq$ . This results in a little larger difference in  $^2T_{2g}$ . We have to pay attention to this type of error enhancement mechanism, that is, small differences in parameters can cause large errors. We show the Tanabe-Sugano diagrams for other TM ions in the Supplemental Material (Figs. S11–S16) [38].

### B. Calculated parameter of free ions

To have a better understanding of Table I, we have applied our method to free TM ions. See computational settings in Sec. II A. Since we have no CF, we set  $Dq = D\sigma = D\tau = 0$ .

Figures 2(e)–2(g) show  $F_0$ ,  $F_2$ , and  $F_4$  for  $\text{TM}^{2+}$  and  $\text{TM}^{3+}$  together with experimental values [45]. Our results follow the Hund rule.  $F_0$  shows a monotonic increase along the

atomic number for the former half up to  $d^4$  as Fig. 2(a). This monotonic behavior is due to two contributions, the orbital shrinkage and the screening effect in the RPA. The size of  $F_0$  is completely different from the case of  $\alpha\text{-Al}_2\text{O}_3\text{:TMs}$  due to the screening effect.

Our calculation for  $F_2$  based on QSGW80 reproduced the experimental values very well especially from  $d^3$  to  $d^7$ . This will support the reliability of our method. On the other hand, we have some systematic disagreements for  $F_4$ : we see a jump between the former half and the latter half. We have no definite idea to explain the disagreements.  $F_2$ 's in  $\alpha\text{-Al}_2\text{O}_3$  are a little lower than free ions because of anisotropic screening effects.

## IV. SUMMARY

We have developed a new method to determine parameters in the effective Hamiltonian of  $3d$  electrons for the  $\alpha\text{-Al}_2\text{O}_3\text{:TMs}$  based on the results of QSGW80. Determined parameters are consistent with experimental results. Moreover, our method was able to predict some reasonable systematic trends of effective interactions in  $\alpha\text{-Al}_2\text{O}_3$  as well as in the TM free ion states, and the reduction of effective Coulomb parameters in  $\alpha\text{-Al}_2\text{O}_3$  compared to those of the free ion.

However, we have faced some problems of hybridization of TM  $3d$  orbitals with  $2p$  orbitals of surrounded oxygen atoms, insufficient information to determine parameters, and shifts of  $10Dq$  due to background charge. For constructing a more precise model, the effect of  $2p$  orbitals of oxygen atoms around TM ions should be included as a self-energy in the

future. Consideration of delocalization effects may improve especially the estimation of CF parameters.

We evaluated the mechanism of numerical errors as shown in Fig. 3. A little numerical difference in the parameters can change the energy ordering of multiplets. This may indicate that our method should be combined with some data assimilation techniques for obtaining reliable results for CMD.

## ACKNOWLEDGMENTS

This work was partly supported by JSPS KAKENHI (Grants No. 20K05303, No. 18H05212, No. 22K04909, No. 23H05449, and No. 23H05457), JST CREST (Grant No. JPMJCR18I2), and JST, the establishment of university fellowships towards the creation of science technology innovation (Grant No. JPMJFS2125).

- 
- [1] G. Blasse and A. Brill, *Appl. Phys. Lett.* **11**, 53 (1967).
- [2] H. Watanabe, H. Wada, K. Seki, M. Itou, and N. Kijima, *J. Electrochem. Soc.* **155**, F31 (2008).
- [3] J. W. Moon, B. G. Min, J. S. Kim, M. S. Jang, K. M. Ok, K.-Y. Han, and J. S. Yoo, *Opt. Mater. Express* **6**, 782 (2016).
- [4] T. Murata, T. Tanoue, M. Iwasaki, K. Morinaga, and T. Hase, *J. Lumin.* **114**, 207 (2005).
- [5] S. Zhang and Y. Hu, *J. Lumin.* **177**, 394 (2016).
- [6] R. Cao, Z. Shi, G. Quan, T. Chen, S. Guo, Z. Hu, and P. Liu, *J. Lumin.* **188**, 577 (2017).
- [7] S. Kück, *Appl. Phys. B* **72**, 515 (2001).
- [8] T. H. Maiman, *Nature* **187**, 493 (1960).
- [9] H. Suzuki, O. Kuribayashi, and F. Kannari, *Opt. Lett.* **22**, 1710 (1997).
- [10] C. A. Morrison, *Crystal Fields for Transition-Metal Ions in Laser Host Materials* (Springer, Berlin, 1992).
- [11] W. Lu, X. Y. Kuang, K. W. Zhou, and D. Die, *J. Phys. Chem. Solids* **65**, 1147 (2004).
- [12] W. L. Yu and J. Z. Wang, *Phys. Status Solidi B* **176**, 433 (1993).
- [13] S. Sugano and I. Tsujikawa, *J. Phys. Soc. Jpn.* **13**, 899 (1958).
- [14] W. M. Fairbank, G. K. Klauminzer, and A. L. Schawlow, *Phys. Rev. B* **11**, 60 (1975).
- [15] I. Shavitt, The method of configuration interaction, in methods of electronic structure theory, in *Modern Theoretical Chemistry*, edited by H. F. Schaefer (Plenum, New York, 1977).
- [16] S. Ohnishi and S. Sugano, *Jpn. J. Appl. Phys.* **21**, L309 (1982).
- [17] X Shangda, G. Changxin, L. Libin, and D. E. Ellis, *Phys. Rev. B* **35**, 7671 (1987).
- [18] W. Duan, G. Paiva, R. M. Wentzcovitch, and A. Fazzio, *Phys. Rev. Lett.* **81**, 3267 (1998).
- [19] H. U. Rahman and W. A. Runciman, *J. Phys. C* **4**, 1576 (1971).
- [20] M. Dong-ping, M. Xiao-dong, C. Ju-rong, and L. Yan-yun, *Phys. Rev. B* **56**, 1780 (1997).
- [21] K. Ogasawara, T. Ishii, I. Tanaka, and H. Adachi, *Phys. Rev. B* **61**, 143 (2000).
- [22] M. Novita and K. Ogasawara, *J. Phys. Soc. Jpn.* **81**, 104709 (2012).
- [23] K. Ogasawara, K. C. Mishra, and J. Collins, *ECS J. Solid State Sci. Technol.* **9**, 016011 (2020).
- [24] K. Suzuki, T. Kotani, and K. Sato, *Phys. Rev. Res.* **5**, 013111 (2023).
- [25] Y. Kitaoka, K. Nakamura, T. Akiyama, T. Ito, M. Weinert, and A. J. Freeman, *Phys. Rev. B* **87**, 205113 (2013).
- [26] S. Na-Phattalung, S. Limpijumnong, and J. T-Thienprasert, *Phys. Status Solidi B* **257**, 2000159 (2020).
- [27] M. W. Haverkort, M. Zwierzycki, and O. K. Andersen, *Phys. Rev. B* **85**, 165113 (2012).
- [28] R. O. Kuzian, O. Janson, A. Savoyant, J. van den Brink, and R. Hayn, *Phys. Rev. B* **104**, 085154 (2021).
- [29] M. van Schilfhaarde, T. Kotani, and S. Faleev, *Phys. Rev. Lett.* **96**, 226402 (2006).
- [30] T. Kotani, M. van Schilfhaarde, and S. V. Faleev, *Phys. Rev. B* **76**, 165106 (2007).
- [31] T. Kotani and M. van Schilfhaarde, *Phys. Rev. B* **81**, 125117 (2010).
- [32] D. Deguchi, K. Sato, H. Kino, and T. Kotani, *Jpn. J. Appl. Phys.* **55**, 051201 (2016).
- [33] H. Sakakibara, T. Kotani, M. Obata, and T. Oda, *Phys. Rev. B* **101**, 205120 (2020).
- [34] T. Kotani and M. van Schilfhaarde, *J. Phys.: Condens. Matter* **20**, 295214 (2008).
- [35] H. Okumura, K. Sato, and T. Kotani, *Phys. Rev. B* **100**, 054419 (2019).
- [36] P. Giannozzi *et al.*, *J. Phys.: Condens. Matter* **21**, 395502 (2009).
- [37] P. Giannozzi *et al.*, *J. Phys.: Condens. Matter* **29**, 465901 (2017).
- [38] See Supplemental Material at <http://link.aps.org/supplemental/10.1103/PhysRevB.108.035141> for details of the structure optimizations, the electronic structures, and the multiplet energy structures for all systems, which includes Refs. [40,41].
- [39] <http://github.com/tkotani/ecalj>.
- [40] R. D. Shannon, *Acta Cryst.* **A32**, 751 (1976).
- [41] J. A. Aramburu, P. Garcia-Fernandez, J. M. Gracia-Lastra, M. T. Barriuso, and M. Moreno, *Phys. Rev. B* **85**, 245118 (2012).
- [42] K. W. H. Stevens, *Proc. Phys. Soc. London Sect. A* **65**, 209 (1952).
- [43] E. König and S. Kremer, *Ligand Field Energy Diagrams* (Springer, Erlangen, 1977).
- [44] E. U. Condon and G. H. Shortley, *Phys. Rev.* **37**, 1025 (1931).
- [45] S. Sugano, Y. Tanabe, and H. Kamimura, *Multiplets of Transition-Metal Ions in Crystal* (Academic Press, London, 1970).
- [46] A. I. Liechtenstein, V. I. Anisimov, and J. Zaanen, *Phys. Rev. B* **52**, R5467(R) (1995).
- [47] I. Souza, N. Marzari, and D. Vanderbilt, *Phys. Rev. B* **65**, 035109 (2001).
- [48] M. L. Bortz and R. H. French, *Appl. Phys. Lett.* **55**, 1955 (1989).
- [49] E. Feher and M. D. Sturge, *Phys. Rev.* **172**, 244 (1968).
- [50] J. Pontnau and R. Adde, *J. Phys. France* **37**, 603 (1976).
- [51] M. Açıkgöz, *Opt. Mater.* **34**, 1128 (2012).



- [52] W.-C. Zheng, X.-X. Wu, W. Fang, and Y. Mei, *Spectrochim. Acta Part A* **66**, 1295 (2007).
- [53] W. Fang, Q. W. Wang, W. Y. Yang, and W. C. Zheng, *Physica B* **408**, 169 (2013).
- [54] P. F. Moulton, *J. Opt. Soc. Am. B* **3**, 125 (1986).
- [55] S. Kammoun, H. Soussi, R. Maalej, M. Dammak, and M. Kamoun, *J. Lumin.* **129**, 411 (2009).
- [56] Our original code for the parameter determination and the exact diagonalization is available at <https://github.com/ktszk/eigloc>.
- [57] M. O. J. Y. Hunault *et al.*, *J. Phys. Chem. A* **122**, 4399 (2018).
- [58] J. Y. Wong, M. J. Berggren, and A. L. Schawlow, *J. Chem. Phys.* **49**, 835 (1968).
- [59] J. Pontnau and R. Adde, *Phys. Rev. B* **14**, 3778 (1976).